

1 Mach Number Correction of Rectangular 2 Duct Criticals

3
4 **Dave Bartran**

5 dbartran@primary.net

6 ASME Member

7
8 **Gregory Banyay**

9 gab5631@psu.edu

10 ASME Member

11 12 **ABSTRACT**

13 *The theory involved in accounting for the velocity dependence of acoustic cut-off frequencies in*
14 *rectangular ducts is briefly summarized. This is followed by a comparison with reported duct critical*
15 *frequencies in a flow test involving isolated cylinders in cross-flow. The agreement with the theory*
16 *illustrates the importance of addressing the Mach number effects in moderate to high velocity services.*

17 18 **INTRODUCTION**

19
20 The role of fluid velocity in formulating duct mode resonances, often referred to
21 as the cut-off frequencies in isentropic uniform flow is well known, and readily
22 developed from the convected wave equations [1-5]. While it is of little importance for

23 fluid velocities less than 40 m/s as in air ducting and many heat exchanger applications,
24 published flow test in [6] covering a range of Mach numbers of 0.1 - 0.4, illustrate its
25 potential significance. Operating experience in power plants likewise suggests the
26 importance of understanding acoustic resonance conditions in steam lines [7], yet is not
27 directly addressed in current industry guidance [8].

28 The flow tests presently under consideration [6], rely on carefully arranged,
29 isolated cylinders in uniform, low turbulence cross-flow, to excite the acoustic duct
30 modes sequentially as the fluid velocity is increased. This allows us to carefully examine
31 the velocity dependence of the duct modes excited, with identifiable near constant
32 Strouhal numbers of the cylinders of the providing the acoustic excitation.

33

34 DUCT CUT-OFF FREQUENCIES

35

36 The convected wave equations [1-5] involving the acoustic velocity potential or
37 the linearized Euler equations, are used to quantify duct cut-off frequencies or
38 resonances. In rectangular ducts, the velocity potential ϕ , as in [2] is described by

39

$$\frac{\partial^2 \phi}{\partial x^2} + \frac{\partial^2 \phi}{\partial y^2} + \frac{\partial^2 \phi}{\partial z^2} = \frac{1}{c_0^2} \left(\frac{\partial}{\partial t} + v_x \frac{\partial}{\partial x} \right)^2 \phi \quad (1)$$

40 The right hand side of (1) is based on the total derivative of the velocity potential in the
41 presence of idealized uniform flow, with duct coordinates $\{x,y,z\}$, mean fluid
42 velocity V_x , and speed of sound, c_0 .

43 Expanding the total derivative in (1), we now have

$$44 \quad \frac{\partial^2 \phi}{\partial x^2} + \frac{\partial^2 \phi}{\partial y^2} + \frac{\partial^2 \phi}{\partial z^2} = \frac{1}{c_0^2} \left(\frac{\partial^2 \phi}{\partial t^2} + 2V_x \frac{\partial^2 \phi}{\partial t \partial x} + V_x^2 \frac{\partial^2 \phi}{\partial x^2} \right) \quad (2)$$

45 This equation is combined with the trial solutions in (3) that are periodic in both time
46 and duct coordinates, with frequency ω , and wave numbers $\{k_x, k_y, k_z\}$.

$$47 \quad \phi = A e^{j(k_x x - \omega t)} \cos(k_y y) \cos(k_z z) \quad (3)$$

48 With the duct length considerably greater than the transverse dimensions, we shall
49 focus on the transverse modes. Applying hard-wall boundary conditions given by

$$50 \quad \left. \frac{\partial \phi(x, y, z)}{\partial y} \right|_{y=\pm H/2} = 0 \quad \text{and} \quad \left. \frac{\partial \phi(x, y, z)}{\partial y} \right|_{z=\pm W/2} = 0, \quad (4)$$

51 to the trial solutions in (3) requires $k_y = m\pi/H$ and $k_z = n\pi/W$, with integer mode
52 numbers $\{m, n\}$.

53 Substituting the trial solutions into the convected wave equation (2) and
54 simplifying, results in the characteristic equation

55
$$(k_x^2 + k_y^2 + k_z^2) + [(\omega - V_x k_x)^2 / c_0^2 - k_x^2] = 0 \quad (5)$$

56 Upon defining $\beta_{m,n}^2 \equiv k_y^2 + k_z^2$, and rearranging allows us to write

57
$$(1 - M^2)k_x^2 + 2k_x M(\omega/c_0) - [(\omega/c_0)^2 + \beta_{m,n}^2] = 0, \quad (6)$$

58 which is readily solved, yielding the longitudinal wave number as

59
$$k_x(m,n) = -(M\omega/c_0) / \sqrt{1 - M^2} \pm \sqrt{(\omega/c_0)^2 - \beta_{m,n}^2 / (1 - M^2)} \quad (7)$$

60 When k_x is real, longitudinal propagation is allowed, and cut-off (or attenuated)

61 otherwise.

62 In the absence of flow, the wave number $k_x(m,n)$ is zero for $\omega/c_0 = \beta_{m,n}$, with

63 propagation cut-off at the traditional duct resonance condition

64
$$\omega(m,n) = c_0 \pi \sqrt{(m/H)^2 + (n/W)^2} \quad (8)$$

65 In the presence of uniform flow, the cut-off frequency is now

66
$$\omega(m,n) = c_0 \pi \sqrt{(n/H)^2 + (m/W)^2 / (1 - M^2)^{0.5}}, \quad (9)$$

67 with wave propagation allowed for $\omega > \omega(m,n)$.

68 Before comparing these predictions with those observed in [6], one can consider a

69 finite element solution of the acoustic wave equation in terms of the acoustic pressure

70 in the absence of flow as in [6]. The Helmholtz pressure wave equation is

71
$$\frac{\partial^2 p}{\partial x^2} + \frac{\partial^2 p}{\partial y^2} = \frac{1}{c_0^2} \frac{\partial^2 p}{\partial t^2} \quad (10)$$

72 With solutions of the form $p = \varphi e^{-j\omega t}$, now (10) reduces to

73
$$\nabla^2 \varphi + k^2 \varphi = 0 \quad (11)$$

74 where $k = \omega/c_0$, with duct cut-off frequencies ω , and speed of sound c_0 . Using (11)

75 together with the hardwall boundary conditions $\varphi(x, y)|_{y=\pm H/2} = 0$ and $\varphi(x, y)|_{z=\pm W/2} = 0$, one

76 can compute the cut-off frequencies ω , and mode shapes φ , using finite element

77 methods described in [9,10].

78

79 FLOW TEST COMPARISON

80

81 The duct dimensions used in the flow test [6] are shown in Fig. 1, with transverse

82 dimensions of the duct width $W=127$ mm and height $H=254$ mm, with cylinders having

83 diameter $D=12.7$ mm. The reported Strouhal number as $St(m, 0) = D f(m, 0) / V$, is taken

84 as the mean of those reported in Table 1 of [6] as $St=0.189$ for Reynolds number of

85 31,000 to 137,000. This Strouhal estimate agrees with the empirical correlations in [11]

86 commonly used with smooth cylinders in cross flow. The fluid temperature is not

87 stated, so we have assumed it to equal 20 degrees C, which corresponds to $c_0=343$ m/s.

88 The reported duct resonances presented in Table 1, represent single and

89 multiple cylinders, which are carefully positioned to coincide with the acoustic particle

90 velocity antinodes, so as to engage the first three duct modes in sequential fashion with
91 increasing fluid velocity. The frequencies reported for a given mode number are
92 averaged to provide mean estimates of each frequency of each mode. The root mean
93 square (RMS) of the fluctuations about the mean are less than 0.5% for each mode. In
94 the case of the single cylinder located midway at $y/H=0$ (a pressure node), the $m=2$
95 mode is not excited, and is omitted from the averaging process. The changes in the
96 absolute temperature associated with the reported pressure drop are less than 0.22% at
97 100 m/s and 0.58% at 150 m/s, and is omitted from consideration.

98 The mean duct criticals for the half-dozen cylinder arrangements tested, are
99 plotted in Fig. 2, versus the transverse mode number m , with and without the Mach
100 number correction. The finite element calculations, shown as a dashed line, coincide
101 with the analytical solutions in (8). The fluid velocity associated with the modes excited
102 by vortex shedding acoustics is shown adjacent to the mode number to facilitate
103 association of the fluid velocity and this cylinder shedding rate associated with the
104 modes excited.

105 In Table 1, the predicted duct criticals (9) versus mode number together with the
106 mean fluid velocity at each excited duct resonance are summarized together with the
107 frequency deviation from the mean for each mode. Clearly the transverse duct
108 resonances, based on the convected wave equation agree with the flow test data. The
109 criticals without the Mach number correction, over-estimate those observed by 0.4% for

110 velocities of 45 m/s ($M=0.13$), increasing to 7.5% at 127 m/s ($M=0.37$). This suggests
111 that the Mach number correction is minimal in most industrial applications.

112

113 CONCLUSIONS

114

115 This rather brief comparison of the duct criticals intends to increase awareness
116 of the convected wave equation where high velocity fluids are encountered. We began
117 with the convective wave equation in (1) and the transverse resonance conditions in (9),
118 with and without the Mach number correction to exemplify the importance of the Mach
119 number in moderate to high velocity, duct acoustics.

120 While the flow test considered herein specifically to an atmospheric wind tunnel
121 test, it provides definitive evidence of Mach number effects with increasing velocity,
122 thus serving to validate the analysis. The convected wave equation may also be
123 expressed in terms of acoustic pressure and particle velocity, but requires careful
124 attention to the boundary conditions when less than ideal flow conditions are present.
125 Applications involving high velocity fluids in cylindrical ducts are covered in [1-5], while
126 those involving cross-flow heat exchangers as in [12,13] are beyond the scope of the
127 present article and subject to ongoing study.

128

129

130 **REFERENCES**

- 131 [1] Mason, V. (1969) "Some Experiments on the Propagation of Sound Along a
132 Cylindrical Duct Containing Flowing Air," J. Sound Vibr. **10**(2), pp. 208-226.
133 doi.org/10.1016/0022-460X(69)90197-7
- 134 [2] Reinstra, S. W. , Hirscheberg, A. (2021) "An Introduction to Acoustics," Technische
135 Universiteit Eindhoven. Chapter 9. www.win.tue.nl/~sjoerdr/papers/boek.pdf
- 136 [3] Ju, Hongbin, (2009) "Duct Acoustics" www.math.fsu.edu/~hju/index_cht16.html.
- 137 [4] Howe, M.S. (1998) "Acoustics of Fluid Structure Interactions," Cambridge Univ. Press,
138 New York, pp.33-39. ISBN 978-0-521-05428-7.
- 139 [5] John, J.E.A. (1969) "Gas Dynamics," Allyn and Bacon, Boston, p.295. ISBN 0-205-
140 02262-6.
- 141 [6] Arafa, Nadim (2016) "Flow-Excited Acoustic Resonance of Isolated Cylinders
142 in Cross-Flow," ASME J. Press. Vessel Tech., **138**(1): 01130. doi.org/10.1115/1.4030270.
- 143 [7] Hambric, S. A., Ziada, S., and Morante, R. J. "Overview of Boiling Water Reactor
144 Steam Dryer Alternating Stress Assessment Procedures." ASME J. of Nuclear Rad Sci.
145 April 2018; **4**(2): 021002. doi.org/10.1115/1.4037898
- 146 [8] ASME. "Boiler and Pressure Vessel Code, Section III," 2023.
- 147 [9] Kinsler, L., Frey, A.R., Coppens, A. B., Sanders, J.V., (1982) "Fundamentals of
148 Acoustics," 3rd Edition, Wiley, New York. ISBN 10-0471029335.
- 149 [10] Hughes, T.J.R. (2000) "The Finite Element Method: Linear Static and Dynamic Finite
150 Element Analysis," Dover Pub. Mineola, NY. ISBN 10-0486411818.[11] Blevins, R. D.
151 (2009) "Models for Vortex-Induced Vibration of Cylinders Based on Measured Forces,"
152 ASME J. Fluids Eng., **131**(10): 101203. doi.org/10.1115/1.3222906.
- 153 [12] Hamakawa, H., Fukano, T., Nishida, E., Ishida, H. (2006) "Effect of Flow Induced
154 Acoustic Resonance on Vortex Shedding from Staggered Tube Banks," JSME Int'l J. Series
155 B Fluids and Thermal Eng., **49**(1), pp.142-151, doi.org/10.1299/jsmeb.49.142
- 156 [13] Mohany, A., Alziadeh, M., and Hassan, M. (2023) "Vorticity Shedding and Acoustic
157 Resonance Excitation of a Square Tube Array: Effect of Flow Approach Angle," ASME. J.
158 Press. Vessel Tech., **145**(1): 011401. doi.org/10.1115/1.4055158

159

160

Figure Captions List

161

Fig. 1 Duct Coordinates showing side and end view and representative cylinder placements in [6]

Fig. 2 Comparison of duct criticals with and without uniform flow Mach No. correction

162

Accepted Manuscript Not Copyedited

163

Table Caption List

164

Table 1 Frequency of transverse duct modes for single and multiple cylinders [6]

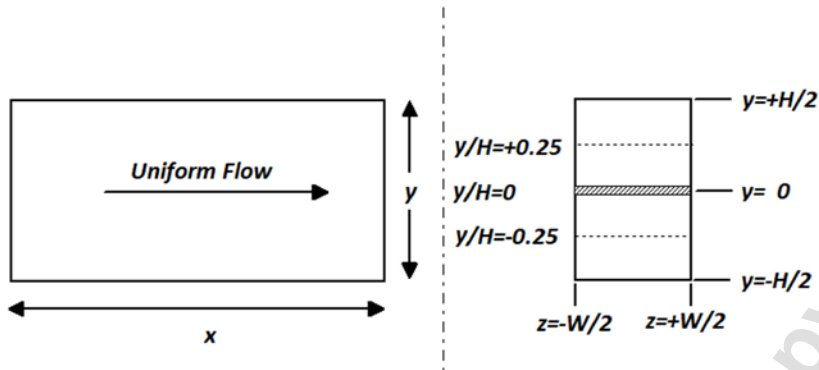
165

166

Accepted Manuscript Not Copyedited

167

Fig. 1



168

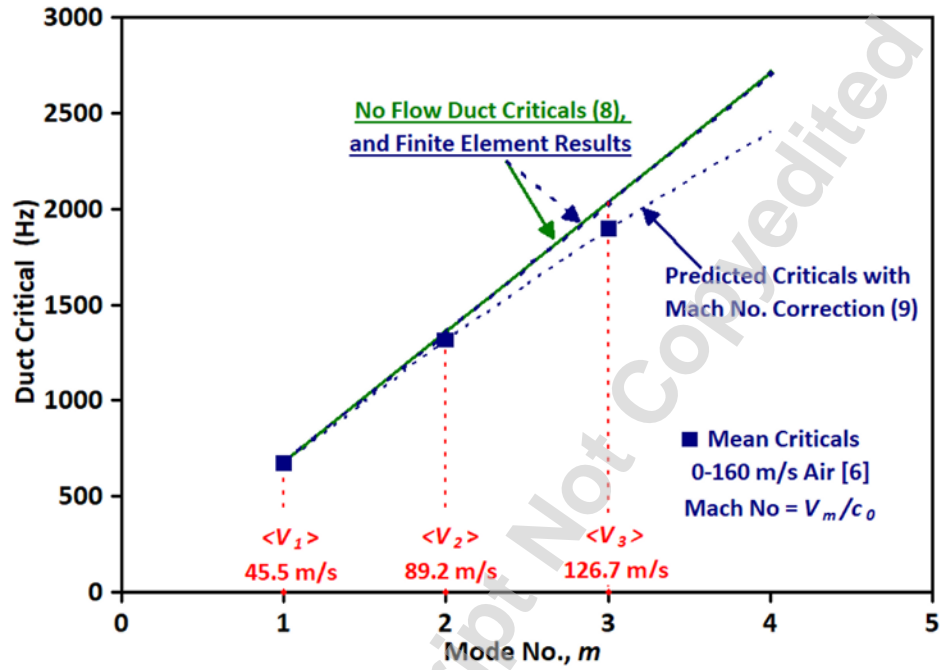
Accepted Manuscript Not Copied

Downloaded from <http://memagazine.asmedigitalcollection.asme.org/pressure-vesseltech/article-pdf/doi/10.1115/1.4067726/7426247/pv-24-1150.pdf> by guest on 26 April 2025

169

170

Fig. 2



171

172

Table 1

<u>Y/H Cylinder</u> <u>Location</u>	<u>First Transverse</u> <u>Mode;</u> <u>Mach=0.131</u> <u>m=1</u>	<u>Second Transverse</u> <u>Mode;</u> <u>Mach=0.259</u> <u>m=2</u>	<u>Third Transverse</u> <u>Mode;</u> <u>Mach=0.370</u> <u>m=3</u>	<u>St Nos.</u> <u>Reported</u> <u>m=1; n=0</u>
-	(Hz)	(Hz)	(Hz)	-
0	678	<u>Not excited</u>	1884	0.190
0.25	681	1326	1886	0.189
0 , 0.25	679	1332	1889	0.193
0.25 , -0.25	678	1324	1880	0.194
0, 0.25 & -0.25	679	1332	1879	0.187
0, 0.167 & -0.167	677	1326	1926	0.184
RMS Scatter	<u>0. 1%</u>	<u>0.1%</u>	<u>0.4%</u>	<u>0.7%</u>
$\langle f(m,n)=0 \rangle$	<u>679</u>	<u>1330</u>	<u>1891</u>	<u>0.189</u>

173